ELSEVIER

Journal of Photochemistry and Photobiology A: Chemistry 98 (1996) 121–126

Journal of PHOTOCHEMISTRY AND PHOTOBIOLOGY A:CHEMISTRY

Suppression of the harpooning mechanism in donor–bridge–acceptor systems by aza substitution in the bridge

Xavier Y. Lauteslager, Bas Wegewijs, Jan W. Verhoeven, Albert M. Brouwer *

Laboratory of Organic Chemistry, Amsterdam Institute of Molecular Studies, University of Amsterdam, Nieuwe Achtergracht 129, NL-1018 WS Amsterdam, Netherlands

Received 19 September 1995; accepted 9 November 1995

Abstract

An aza substituent was introduced in the bridge of donor–bridge–acceptor systems known to undergo harpooning (long-range photoinduced charge separation followed by electrostatically driven folding). Although the substitution does not reduce the conformational flexibility of the bridge, it fully suppresses the harpooning mechanism. From a comparison with a reference compound, the solvatochromic shifts of charge transfer fluorescence and transient absorption results, it is concluded that suppression is due to the low ionization potential of the aza substituent, which leads to a strong reduction of the positive charge on the terminal donor in the excited state.

Keywords: Photoinduced electron transfer; Intramolecular charge-transfer states; Conformational dynamics; Solvent effects; Emission solvatochromic

1. Introduction

Recently, we have presented the synthesis and photophysical properties of compounds **1a** and **1b** [1] (Scheme 1). In non-polar media and in the gas phase, the photophysics of these donor–bridge–acceptor compounds can be described by the transitions outlined in Fig. 1.

Excitation to the locally excited state of the cyanonaphthalene acceptor is followed by intramolecular charge separation in an extended conformation to yield an extended charge transfer (ECT) state with a charge separation distance of approximately 5 Å. The positive charge on the aniline donor and the negative charge on the cyanonaphthalene acceptor are attracted to one another by coulombic forces. In media of low dielectric constant, this induces a dramatic conformational change. The most pronounced feature of this is that the piperidine ring changes from the chair conformation, preferred in the ground state, to a boat conformation. Combined with additional rotation around the bonds linking the cyanonaphthalene acceptor to the piperidine ring, this leads to a reduction of the donor–acceptor distance to approximately 3 Å and a so-called compact charge transfer (CCT) state [2] is formed. Evidence for this "harpooning" mechanism was obtained from temperature-dependent and time-resolved fluorescence measurements in solution and in a solid matrix [3], supersonic jet spectroscopy [4] and time-resolved microwave conductivity (TRMC) measurements [1].

In this paper, we study the effect of the introduction of a heteroatom in the bridge between the chromophores. In compounds **2a** and **2b**, this is realized via replacement of the

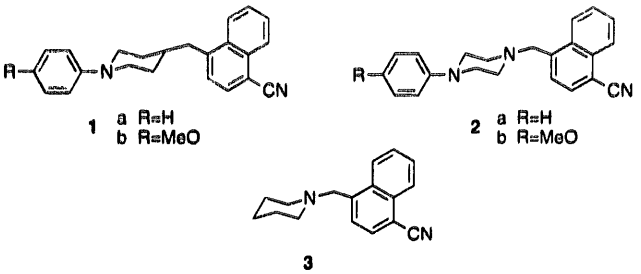

Scheme 1.

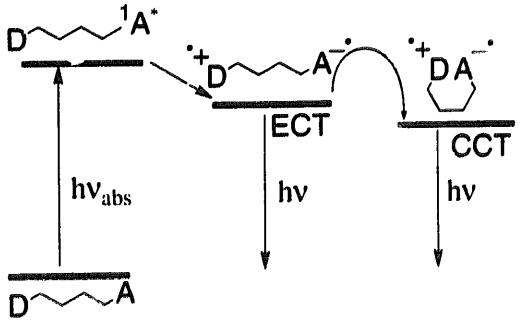

Fig. 1. Schematic representation of the harpooning process.

* Corresponding author. Tel.: 31 20 5255491; fax: 31 20 5255670; e-mail: fred@org.chem.uva.nl.

SSDI 1010-6030(95)04276-8

piperidine ring by a piperazine ring. The conformational potential energy surfaces for ring inversion are not dramatically different for these heterocyclic six-membered rings, but an additional folding pathway exists in the piperazine derivatives, namely inversion of the saturated amino group. It should be noted that, via aza substitution, an extra donor group is also introduced; we can therefore consider the systems as trichromophoric compounds [5] with a cyanonaphthalene acceptor (A), a trialkyl nitrogen as the first donor (D_1) and a stronger (methoxy)aniline donor as the second donor (D_2). For comparison, compound **3** (D_1–A) was also included in the study.

2. Results and discussion

2.1. Solvent dependence of CT emission: nature of the CT states

By analogy with **1**, compounds **2** and **3** display no local emission of the separate chromophores. Instead, in all solvents, a broad solvatochromic emission is observed which is attributed to CT fluorescence. The emission maxima determined in different solvents are given in Table 1. The fluorescence quantum yields (Φ_f) of compounds **2a**, **2b** and **3** are substantially lower in all solvents than those of compounds **1a** and **1b** (in cyclohexane, Φ_f(**1a**) = 0.20, Φ_f(**1b**) = 0.05, Φ_f(**2a**) = 0.01, Φ_f(**2b**) = 0.02, Φ_f(**3**) ≪ 0.01).

The solvent dependence of the CT fluorescence can be analysed on the basis of dielectric continuum theory, using the well-known Lippert–Mataga equation [7]

$$\tilde{\nu}_{CT} = \tilde{\nu}_{CT}(0) - \frac{2\mu_{CT}^2}{hc\rho^3}\Delta f = \tilde{\nu}_{CT}(0) - 10070\frac{\mu_{CT}^2}{\rho^3}\Delta f \quad (1)$$

$$\Delta f = \frac{(\epsilon_s - 1)}{(2\epsilon_s + 1)} - \frac{(n^2 - 1)}{(4n^2 + 2)} \quad (2)$$

In this equation, the solvent dependence of the CT emission wavenumber $\tilde{\nu}_{CT}$ is correlated with the solvent polarity parameter Δf (Eq. (2)), where $\tilde{\nu}_{CT}(0)$ (cm^{-1}) is the emission maximum in the gas phase, μ_{CT} (D) is the dipole moment of the CT state, h is Planck's constant, c is the velocity of light, ρ (Å) is the effective radius of the solvent cavity occupied by the molecule, ϵ_s is the solvent dielectric constant and n is its refractive index. Fig. 2(a) shows the Lippert–Mataga plots of **1a** and **1b**.

As reported earlier [8], the data for **1a** and **1b** cannot be fitted by a single straight line. Instead, two discrete linear regions can be distinguished, one with a larger slope (in polar solvents and at low temperature in non-polar solvents, triangles) and one with a smaller slope (in non-polar solvents, circles). Thus the dipole moment of the emissive species is not the same over the solvent polarity region studied. An explanation in terms of two distinctly different species, ECT and CCT states, is offered by the harpooning mechanism (Fig. 1): in non-polar solvents, a conformational change from an extended (ECT) to a compact (CCT) structure is induced by the electrostatic attraction between D^+ and A^-, whereas in more polar solvents the dielectric screening attenuates this driving force, allowing the ECT species to survive. As mentioned in Section 1, strong evidence for this mechanism has been gathered from time-resolved and temperature-dependent fluorescence measurements, fluorescence measurements in a solid matrix, TRMC measurements and supersonic jet spectroscopy. Fig. 2(a) also shows that the lines of **1b** are shifted to lower energy relative to **1a**, which indicates a lowering of the CT state by approximately 0.25 eV on introduction of the stronger methoxyaniline donor. The experimental parameters obtained from fitting the data according to Eq. (1) ($2\mu^2/hc\rho^3$ and $\tilde{\nu}_{CT}(0)$) are given in Table 2.

From the fits, the dipole moments of both CT states can be estimated. Using a cavity radius (ρ) of 5.4 Å [9], dipole

Table 1
Solvent dependence of charge transfer fluorescence maxima (10^3 cm^{-1})

Solvent	ϵ [a]	Δf [b]	1a	1b	2a	2b	3
Gas phase		0	23.0	21.5	–	–	–
Methylcyclohexane (low temperature)	–	–	26.0	23.8	–	–	–
Cyclohexane	2.02	0.100	22.1	19.3	20.6	19.7	23.3
Di-*n*-hexylether	2.77	0.170	21.2	18.6	18.7	18.0	21.3
Di-*n*-butylether	3.10	0.194	20.8	18.4	18.5	17.8	21.1
Diethylether	4.20	0.251	20.2	17.5	17.4	16.2	19.6
Butylacetate	5.01	0.267	–	–	–	15.8	–
Ethylacetate	6.02	0.292	17.4	15.7	15.9	15.2	17.5
Tetrahydrofuran	7.58	0.308	17.4	15.5	16.0	15.2	17.5
Dichloromethane	8.93	0.319	17.2	–	15.8	–	–
Acetonitrile	35.9	0.393	–	–	13.5	–	15.6

[a] Dielectric constant [6].
[b] See Eq. (2).

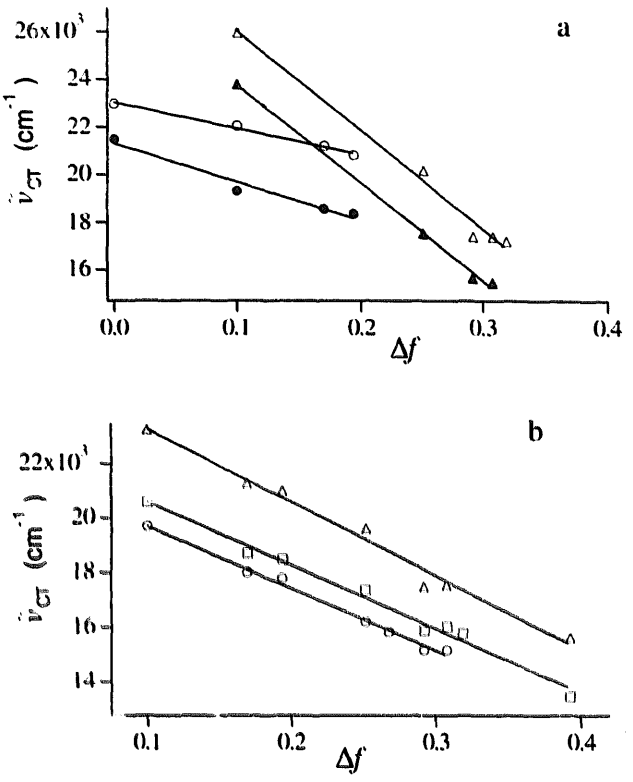

Fig. 2. Fluorescence maximum wavenumber $\tilde{\nu}_{CT}$ (cm^{-1}) in different solvents vs. Δf (see Eq. (1)) for: (a) **1a** (open symbols) and **1b** (filled symbols) (the two data points at $\Delta f = 0.1$ follow from measurements in methylcyclohexane at room temperature and below the melting point of methylcyclohexane); (b) **2a** (squares), **2b** (circles) and **3** (triangles).

moments of 13 and 16 D are calculated for the CCT species of **1a** and **1b** respectively. This corresponds to charge separation distances of 2.7 and 3.3 Å, which are the distances expected for a sandwich-like conformation. The dipole moment of the ECT state is found to be approximately 26 D for both compounds, corresponding to a charge separation distance of 5.3 Å. In contrast with the behaviour of compounds **1a** and **1b**, a linear relation covering the whole polarity range is observed in the Lippert–Mataga plot of **2a** and **2b** (Fig. 2(b)). This indicates that only one CT species is formed and no conformational change takes place in non-polar solvents.

The question remains as to the nature of the CT state observed. In principle, three possibilities can be distinguished. With the reasonable assumption that the negative charge will be located on the cyanonaphthalene acceptor, the positive charge can be located on the trialkyl nitrogen, the aniline nitrogen or delocalized over the two piperazine nitrogens [10]. Compound **3** is a useful reference compound to address this question. This compound shows solvatochromic CT fluorescence in a large range of solvents and obviously only one CT state can be formed. The Lippert–Mataga plot of this compound is also shown in Fig. 2(b). The slopes and

Table 2
Experimental parameters (10^3 cm^{-1}) obtained from the Lippert–Mataga analysis of compounds **1**, **2** and **3**

Parameter	1a	1b	2a	2b	3
$2\mu^2/hc\rho^3$(CCT)	10.9	16.1	–	–	–
$\tilde{\nu}_{CT}(0)$(CCT)	23.1	21.3	–	–	–
$2\mu^2/hc\rho^3$(ECT)	41.4	41.1	23.2	22.8	27.0
$\tilde{\nu}_{CT}(0)$(ECT)	30.2	27.9	22.9	22.0	26.0

intercepts of the linear fits of the CT wavenumber vs. solvent polarity parameter plots are shown in Table 2.

Let us first compare the emission energies of **2a** and **2b**. The latter emits at lower energy. The difference extrapolated to the gas phase is 0.12 eV, which is clearly less than the difference between the oxidation potentials of the D_2 moieties in these compounds, which are 0.81 and 0.61 V for **1a** and **1b** respectively (vs. SCE in acetonitrile [11]). For compounds **1a** and **1b**, the difference in donor strength is reflected by the difference in the gas phase emission energies of approximately 0.25 eV. This indicates that full charge separation from D_2 to A does not occur in the CT states of compounds **2a** and **2b**. On the other hand, the difference between **2a** and **2b** and, more importantly, the difference between **2** and **3** forces us to conclude that a stabilizing interaction must exist between D_2 and the D_1^+–A^- fragment in **2**, which is inevitably associated with a certain transfer of charge to D_2. For the radical cation of *N,N'*-dimethylpiperazine, quantum chemical calculations indicate that the full delocalization of the charge is accompanied by an energy gain of about 0.77 eV [10]. In **2a** and **2b**, the extrapolated gas phase emission energies are lowered by 0.38 and 0.50 eV respectively compared with compound **3**. This suggests that charge delocalization is significant. It should be noted, however, that the emission energies are also affected by the reorganization energies. For the case of *N,N'*-dimethylpiperazine, the internal reorganization energy for the delocalized radical cation is computed to be substantially larger than for the localized radical cation [12]. We may expect that the partial transfer of charge from D_1 to D_2 in the CT states of compounds **2a** and **2b** also leads to a larger reorganization energy relative to the ground state. This will make an additional contribution to the red shift of the emission.

If it is true that some CT to D_2 occurs in the CT state D_2–D_1^+–A^-, the excited state dipole moment of **2a** and **2b** should be greater than that of **3**. The solvatochromic shift of the CT emission of **2a** and **2b** is, however, smaller than that of **3**. This apparent contradiction can be resolved if the reasonable assumption is made that the (partial) charge delocalization in compounds **2a** and **2b** not only leads to a larger dipole moment, but also to a greater effective cavity radius.

2.2. Time-resolved measurements: decay pathways of the CT states

The fluorescence decay times of the CT states of compounds **1**, **2** and **3**, determined in four solvents, are shown in

Table 3
Fluorescence decay times (ns) (for details, see Section 4)

Solvent	1a	1b	2a	2b	3
Cyclohexane	72	38	1.2	2.8	0.3
Di-*n*-butylether	26	18	1.8	3.4	0.4
Diethylether	15	19	1.2	1.7	0.6
Ethylacetate	–	7	0.2	–	0.8

Table 3. Typically, the lifetimes of compounds **1a** and **1b** exceed those of compounds **2** and **3** by more than an order of magnitude, thus supporting the conclusion that the aza substituent in **2** and **3** changes the nature of the emissive CT state. Another difference is observed with respect to the influence of the energy gap separating the CT state and the ground state on the lifetime of the former. For systems **1a** and **1b**, decreasing this energy gap by increasing the donor strength (**1a** → **1b**), or by increasing the solvent polarity, leads to a reduced lifetime of the CT state, consistent with the expected "inverted region" behaviour. For **3**, however, the lifetime increases in more polar solvents, while compounds **2a** and **2b** first show an increase and then a decrease. Also when compounds **2a**, **2b** and **3** are compared with one another in the same solvent, a smaller energy gap (i.e. longer CT fluorescence wavelength) seems to increase the lifetime.

In order to characterize further the decay pathways, transient absorption spectra were measured in cyclohexane, diethylether and tetrahydrofuran. In all solvents, compounds **1a** and **1b** show absorptions characteristic of the (methoxy)aniline radical cation and the cyanonaphthalene radical anion, indicating that the CT state is accessible, in accordance with the steady state fluorescence spectra. Fig. 3 shows the transients for **1b** observed in argon-saturated cyclohexane.

The lifetime determined from the decay of the absorption, using simple exponential fitting of the intensity of either anion or cation bands, corresponds reasonably well with the fluorescence lifetime (31 ns vs. 38 ns). At longer delays, only the triplet–triplet absorption is visible from the cyanonaphthalene acceptor chromophore, which is the lowest local triplet in these compounds (E_T = 2.49 eV). Compounds **2** and **3**, in contrast, show no clear absorption characteristics of the cyanonaphthalene radical anion or radical cations. Instead, only the triplet–triplet absorption of cyanonaphthalene is observed, which decays slowly (Fig. 4).

This observation is in line with the fluorescence lifetimes of **2** and **3** (Table 3), as the time resolution of our transient absorption set-up is limited to approximately 5 ns and the lifetimes of the CT emissions are considerably shorter. As observed previously, intersystem crossing from D^+–A^- (^{1}CT) to ^{3}A can be remarkably fast in amine–CH_2–naphthalene systems [13,14].

Having established that the formation of a triplet acceptor state is the major deactivation pathway for **2** and **3**, we can understand the trends observed in the fluorescence lifetimes of these compounds. Intersystem crossing from ^{1}CT to ^{3}A in this case can be viewed as an electron transfer process occurring in the Marcus normal region. When the energy of the CT state is lowered, by introduction of the second stronger donor, the driving force for intersystem crossing is reduced and, consequently, the rate of this charge recombination process also decreases. Further lowering of the energy of the CT state to bring it below ^{3}A will prevent intersystem crossing, but direct charge recombination to the ground state will be enhanced, which is typical for electron transfer in the inverted region. Indeed, in compound **2b** in tetrahydrofuran, the formation of ^{3}A is not observed. In this solvent, a very weak transient is observed only during the laser pulse (7 ns FWHM). The spectrum, shown in Fig. 5, displays absorption bands which resemble those of the cyanonaphthalene radical anion and the radical cation of methoxyaniline. No triplet–triplet absorption is observed, indicating that the CT state is now too low in energy to be able to cross efficiently to the triplet state. So, in this polar solvent, the fully charge separated state can be observed, although it is very short lived.

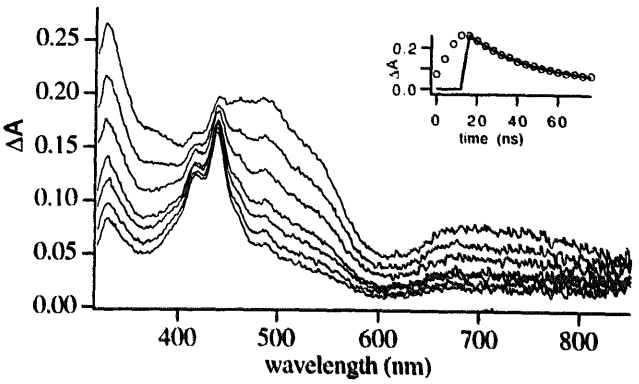

Fig. 3. Transient absorption spectra of **1b** in cyclohexane. The first spectrum (with the highest intensity) was taken at the maximum of the laser pulse (308 nm, 7 ns FWHM), and the subsequent spectra were taken with time increments of 10 ns.

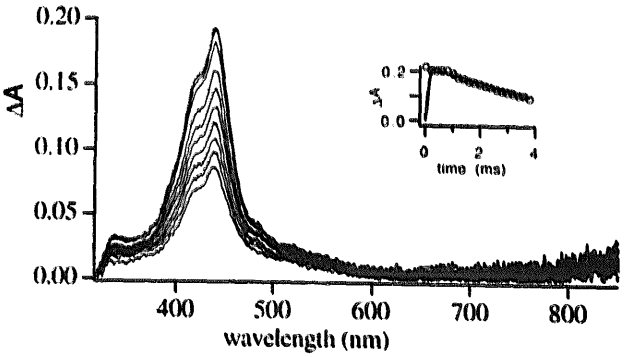

Fig. 4. Transient absorption spectra of **2b** in cyclohexane. The first spectrum (with the highest intensity) was taken at the maximum of the laser pulse, and the subsequent spectra were taken with time increments of 400 ns.

3. Conclusions

Although the trialkyl nitrogen lone pair in compounds **2a** and **2b** is significantly harder to oxidize than the (*p*-methoxy)aniline unit, its presence nevertheless prevents the for-

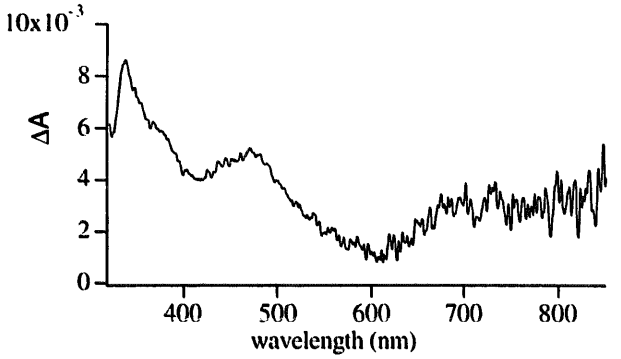

Fig. 5. Transient absorption spectrum of **2b** in tetrahydrofuran observed during the laser pulse (308 nm, 7 ns FWHM).

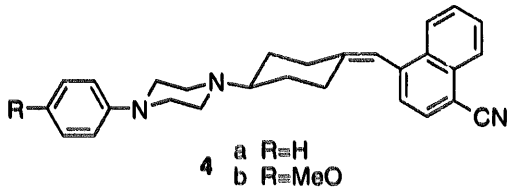

4

Scheme 2.

mation of a CCT state between the cyanonaphthalene acceptor and the aniline donor. This corroborates the harpooning mechanism of CCT ("exciplex") formation in **1a** and **1b**, since the weaker donor properties of the trialkyl nitrogen allow it to interfere with the first step in such a mechanism, i.e. long-range charge separation, because of its shorter distance to the acceptor. Trapping of the positive charge on the trialkyl nitrogen (D_1) prevents the formation of an ECT state (D_2^+–D_1–A^-), thereby also precluding the electrostatically driven folding from ECT to CCT, typical of the harpooning mechanism.

To prevent the trapping of the positive charge on the trialkyl nitrogen, increasing the acceptor strength will have no effect. However, further lowering the ionization potential of the aniline unit should, in principle, allow harpooning to reappear. In this context, it should be noted that Brouwer et al. [15] reported the conformational dynamics of other trichromophoric compounds (**4**, see Scheme 2) with a piperazine moiety.

In this case, it was found that the introduction of the methoxy group in the aniline moiety caused a change in the CT state from D_2–D_1^+–A^- to D_2^+–D_1–A^-. Because of the smaller ratio of the D_2–A and D_1–A distances of **4** compared with **2**, trapping of the charge on D_1 is less favourable. Due to the greater charge on D_2, harpooning can occur in compound **4**.

Experiments to test this approach by modifying systems **2a** and **2b** to include a stronger donor D_2 are currently underway and will be reported separately.

4. Experimental details

4.1. Synthesis

The synthesis of **1a** and **1b** has been reported previously [16].

4.1.1. N-Phenyl-N'-(4-cyano-1-naphthylmethyl)piperazine (2a)

N-Phenylpiperazine (2.44 g, 15.0 mmol) (Janssen, 97%) and 4-bromomethyl-1-naphthonitrile (3.70 g, 15.0 mmol) (synthesized in our laboratory) were stirred for 2.5 h at room temperature in a two-phase system of 15 ml dichloromethane and 15 ml saturated aqueous potassium carbonate solution. The organic layer was dried over sodium sulphate and the solvent was evaporated. Most of the crude product (4 g of the 4.91 g) was recrystallized from a mixture of chloroform and methanol to yield 2.40 g of light-brown crystals. 0.75 g of the 2.40 g was refluxed with activated carbon (Norit) in acetone and, after filtration and evaporation of the solvent, recrystallized from methanol to yield 0.458 g (1.40 mmol, 37%) **2a** as white needles. Melting point, 147–148 °C. IR ($CHCl_3$), $\tilde{\nu}$ (cm^{-1}): 2810 (m), 2220 (m), 1590 (s), 1490 (s). ^1H NMR (200 MHz, $CDCl_3$), δ (ppm): 8.41 (m, 1H), 8.28 (m, 1H), 7.89 (d, 1H, J = 7.3 Hz), 7.67 (m, 3H), 7.27 (m, 2H), 6.90 (m, 3H), 4.02 (s, 2H), 3.21 (t, 4H, J = 5 Hz), 2.70 (t, 4H, J = 5 Hz). ^{13}C NMR (63 MHz, $CDCl_3$), δ (ppm): 151.2, 140.4, 132.6, 132.0, 131.9, 129.0, 128.2, 127.3, 126.0, 125.7, 125.2, 119.7, 117.9, 116.0, 110.0, 60.8, 53.5, 49.3.

4.1.2. N-(4-Methoxyphenyl)-N'-(4-cyano-1-naphthylmethyl)piperazine (2b)

To 3.00 g (11.4 mmol) of *N*-(4-methoxyphenyl)-piperazine dihydrochloride (Aldrich, 90%) in 10 ml of water was added 25 ml of an aqueous 1 M sodium hydroxide solution. The solution was extracted with dichloromethane (5 × 15 ml). The organic layers were dried over sodium sulphate and the solvent was evaporated to yield 1.95 g of a brown oil; 1.58 g of the oil was distilled (in a bulb to bulb apparatus) to give 1.39 g of a white solid, which was used without characterization. The 1.39 g (7.22 mmol) of *N*-(4-methoxyphenyl)piperazine and 1.78 g (7.22 mmol) of 4-bromomethyl-1-naphthonitrile were stirred for 2.5 h in a two-phase system of 7 ml dichloromethane and 7 ml saturated aqueous potassium carbonate solution. After 2 h, extra dichloromethane was added. The organic layer was dried over sodium sulphate and the solvent was evaporated. The crude product (2.62 g) was recrystallized in two fractions from mixtures of chloroform and methanol to yield 1.90 g of yellow/light-brown crystals. 0.90 g of the 1.90 g was refluxed with activated carbon (Norit) in acetone and, after filtration and evaporation of the solvent, recrystallized from methanol to yield 0.584 g (1.63 mmol, 48%) **2b** as off-white needles. Melting point, 161–162 °C. IR ($CHCl_3$), $\tilde{\nu}$ (cm^{-1}): 3000 (m), 2820–2800 (m), 2220 (m), 1575 (w), 1505 (s). ^1H NMR (250 MHz, $CDCl_3$), δ (ppm): 8.39 (m, 1H), 8.26 (m, 1H), 7.86 (d, 1H, J = 7.3 Hz), 7.65 (m, 3H), 6.85 (AA'BB', 4H), 4.00 (s, 2H), 3.75 (s, 3H), 3.08 (t, 4H, J = 5 Hz), 2.68 (t, 4H, J = 5 Hz). ^{13}C NMR (63 MHz, $CDCl_3$), δ (ppm): 153.9, 145.7, 140.5, 132.7, 132.1, 132.0, 128.2, 127.3, 126.0, 125.7, 125.3, 118.2, 117.9, 114.5, 110.0, 60.8, 55.6, 53.6, 50.7.

4.1.3. N-(4-Cyano-1-naphthylmethyl)piperidine (3)

To 1.10 g (4.47 mmol) of 4-bromomethyl-1-naphthonitrile in a 1:1 mixture of diethylether and tetrahydrofuran was added, via a dropping funnel, 1.4 ml (14 mmol) of piperidine in 10 ml of diethylether. The mixture was stirred overnight, water was added (5 ml) and the organic layer was separated. After drying over sodium sulphate and evaporation, almost pure **3** was obtained as a viscous yellow oil. Refluxing with activated carbon in acetone and crystallization from petroleum ether (40–65 °C) yielded 0.180 g (0.72 mmol, 16%) pure **3** as off-white crystals. Melting point, 69–70 °C. IR ($CHCl_3$), $\tilde{\nu}$ (cm^{-1}): 2940 (s), 2850–2800 (m), 2220 (m). ^1H NMR (400 MHz, $CDCl_3$), δ (ppm): 8.38 (m, 1H), 8.25 (m, 1H), 7.85 (d, 1H, J = 7.4 Hz), 7.6 (m, 2H), 7.55 (d, 1H, J = 7.4 Hz), 3.89 (s, 2H), 2.45 (m, 4H), 1.6 (m, 6H). ^{13}C NMR (63 MHz, $CDCl_3$), δ (ppm): 141.4, 132.6, 132.1, 132.0, 128.0, 127.1, 125.7, 125.6, 125.3, 118.1, 109.5, 61.4, 54.9, 26.0, 24.3.

4.2. Measurements

Spectrograde solvents (Merck, Uvasol) were used, except for di-*n*-butylether (Merck, better than 99%, washed three times with H_2SO_4). All ethers were distilled from CaH_2 or $LiAlH_4$ prior to use. Ethylacetate was washed with a saturated Na_2CO_3 solution and distilled from CaH_2. Samples were deoxygenated by bubbling with argon for 15 min.

Fluorescence spectra were taken on a SPEX Fluorolog 2 equipped with a GaAs photomultiplier (RCA C31034, Peltier cooled). Fluorescence lifetimes shorter than 5 ns were measured by time-correlated single photon counting using a Hamamatsu microchannel plate (R3809) detector in a set-up recently described [13], employing a frequency-doubled DCM dye laser synchronously pumped with a mode-locked argon ion laser resulting in 317 nm 19 ps FWHM pulses. Longer lifetimes were measured using a Lumonics EX 700 XeCl excimer laser (308 nm, 7 ns FWHM) and a transient digitizing system. The decay traces were deconvoluted with a computer program (FLD-FIT) using an algorithm developed by Marquardt [17] for non-linear iterative least-square fitting. The quality of the fit was judged from the normalized residuals and χ^2 values. Multiexponential fitting did not improve the quality of the fit. Transient absorption spectra were obtained with a gated optical multichannel analyser (EG&G OMA3) described previously [13]. The excitation source was a Lumonics EX 700 XeCl excimer laser (308 nm) and the probe light (in right-angle geometry) was a 450 W high-pressure Xe arc, pulsed with a Müller Elektronik MSP05 pulser.

Acknowledgements

We greatly appreciate the help of D. Bebelaar (picosecond time-resolved fluorescence) and H.J. van Ramesdonk (transient absorption) and thank P. Gedeck and W. Jäger (Universität Erlangen-Nürnberg) for providing the computer program FLD-FIT. The investigations were supported (in part) by the Netherlands Foundation for Chemical Research (SON) with financial aid from the Netherlands Organization for Scientific Research (NWO).

References

[1] B. Wegewijs, R.M. Hermant, J.W. Verhoeven, M.P. de Haas and J.M. Warman, *Chem. Phys. Lett., 168* (1990) 185.
[2] T. Scherer, I.H.M. van Stokkum, A.M. Brouwer and J.W. Verhoeven, *J. Phys. Chem., 98* (1994) 10 539.
[3] B. Wegewijs, A.K.F. Ng and J.W. Verhoeven, *Recl. Trav. Chim. Pays-Bas, 114* (1995) 6.
[4] B. Wegewijs, A.K.F. Ng, R.P.H. Rettschnick and J.W. Verhoeven, *Chem. Phys. Lett., 200* (1992) 357.
[5] G.F. Mes, H.J. van Ramesdonk and J.W. Verhoeven, *J. Am. Chem. Soc., 106* (1984) 1335.
[6] *Handbook of Chemistry and Physics*, CRC Press, FL, 66th edn., 1986.
[7] E. Lippert, *Z. Naturforsch., Teil A, 10* (1955) 541.
[8] B. Wegewijs, *Ph.D. Thesis*, University of Amsterdam, 1994.
[9] R.M. Hermant, *Ph.D. Thesis*, University of Amsterdam, 1990.
[10] A.M. Brouwer, F.W. Langkilde, K. Bajdor and R. Wilbrandt, *Chem. Phys. Lett., 225* (1994) 386.
[11] T. Scherer, *Ph.D. Thesis*, University of Amsterdam, 1994.
[12] A.M. Brouwer, to be published.
[13] S.I. van Dijk, P.G. Wiering, C.P. Groen, A.M. Brouwer, J.W. Verhoeven, W. Schuddeboom and J.M. Warman, *J. Chem. Soc., Faraday Trans., 91* (1995) 2107.
[14] J. Wirz, personal communication, 1995.
[15] A.M. Brouwer, R.D. Mout, P.H. Maassen van den Brink, H.J. van Ramesdonk, J.W. Verhoeven, S.A. Jonker and J.M. Warman, *Chem. Phys. Lett., 186* (1991) 481.
[16] T. Scherer, W. Hielkema, B. Krijnen, R.M. Hermant, C. Eijckelhoff, F. Kerkhof, A.K.F. Ng, R. Verleg, E.B. van der Tol, A.M. Brouwer and J.W. Verhoeven, *Recl. Trav. Chim. Pays-Bas, 112* (1993) 535.
[17] D.W. Marquardt, *J. Soc. Ind. Appl. Math., 11* (1963) 431.